Proceedings of the
47th IEEE Conference on Decision and Control
Cancun, Mexico, Dec. 9-11, 2008

TuB12.2

# Collective Motion from Consensus with Cartesian Coordinate Coupling - Part II: Double-integrator Dynamics

Wei Ren

*Abstract*— **This is the second part of a two-part paper on collective motion from consensus with Cartesian coordinate coupling. In this part, we study the collective motions of a team of vehicles in 3D by introducing a rotation matrix to an existing consensus algorithm for double-integrator dynamics. It is shown that the network topology, the damping gain, and the value of the Euler angle all affect the resulting collective motions. In particular, we show a necessary and sufficient condition on the damping gain for rendezvous when there is no Cartesian coordinate coupling. We also explicitly show the critical value for the Euler angle when there is Cartesian coordinate coupling and quantitatively characterize the resulting collective motions, namely, rendezvous, circular patterns, and logarithmic spiral patterns. Simulation results are presented to demonstrate the theoretical results.**

## I. INTRODUCTION

Taking into account the fact that equations of motion of a broad class of vehicles require a double-integrator dynamic model, consensus algorithms for double-integrator dynamics are studied in [1]–[6]. In particular, [1], [2] derive conditions on the network topology and the control gains under which convergence is guaranteed. Refs. [3] study formation keeping problems while [4]–[6] study flocking of multiple vehicle systems.

Motivated by [8], we have introduced in the first part [9] of the two-part paper Cartesian coordinate coupling to an existing consensus algorithm for single-integrator kinematics. In this second part, we consider the case of double-integrator dynamics. In contrast to the single-integrator case, the analysis for double-integrator dynamics poses more challenges.

The contributions of this second part of the paper are as follows. We study the convergence properties of a consensus algorithm with a rotation matrix introduced in 3D for double-integrator dynamics over a general network topology. In contrast to the single-integrator case, we show that the network topology, the damping gain, and the value of the Euler angle all play an important role in the resulting collective motions. In particular, we show a necessary and sufficient condition on the damping gain for rendezvous when there is no Cartesian coordinate coupling. We also explicitly show the critical value for the Euler angle when there is Cartesian coordinate coupling and quantitatively characterize the resulting collective motions, namely, rendezvous, circular patterns, and logarithmic spiral patterns. The results generalize the Cartesian coordinate coupling case for single-integrator

W. Ren is with the Department of Electrical and Computer Engineering, Utah State University, Logan, UT 84322, USA
wren@engineering.usu.edu

kinematics presented in [9] to account for dynamic models and also generalize existing consensus algorithms for double-integrator dynamics to achieve different collection motions.

## II. BACKGROUND AND PRELIMINARIES

### A. Graph Theory Notions

It is natural to model interaction among vehicles by directed or undirected graphs. Suppose that a team consists of $n$ vehicles. A weighted graph $\mathcal{G}$ consists of a node set $\mathcal{V} = \{1, \ldots, n\}$, an edge set $\mathcal{E} \subseteq \mathcal{V} \times \mathcal{V}$, and a weighted adjacency matrix $\mathcal{A} = [a_{ij}] \in \mathbb{R}^{n \times n}$. An edge $(i, j)$ in a weighted directed graph denotes that vehicle $j$ can obtain information from vehicle $i$, but not necessarily vice versa. In contrast, the pairs of nodes in a weighted undirected graph are unordered, where an edge $(i, j)$ denotes that vehicles $i$ and $j$ can obtain information from each another. Weighted adjacency matrix $\mathcal{A}$ of a weighted directed graph is defined such that $a_{ij}$ is a positive weight if $(j, i) \in \mathcal{E}$, while $a_{ij} = 0$ if $(j, i) \notin \mathcal{E}$. Weighted adjacency matrix $\mathcal{A}$ of a weighted undirected graph is defined analogously except that $a_{ij} = a_{ji}$, $\forall i \neq j$, since $(j, i) \in \mathcal{E}$ implies $(i, j) \in \mathcal{E}$.

A directed path is a sequence of edges in a directed graph of the form $(i_1, i_2), (i_2, i_3), \ldots$, where $i_j \in \mathcal{V}$. An undirected path in an undirected graph is defined analogously. A directed graph has a directed spanning tree if there exists at least one node having a directed path to all other nodes. An undirected graph is connected if there is an undirected path between every pair of distinct nodes.

Let nonsymmetric Laplacian matrix $\mathcal{L} = [\ell_{ij}] \in \mathbb{R}^{n \times n}$ associated with $\mathcal{A}$ be defined as $\ell_{ii} = \sum_{j=1, j \neq i}^{n} a_{ij}$ and $\ell_{ij} = -a_{ij}$, $i \neq j$. For a weighted undirected graph, $\mathcal{L}$ is symmetric positive semi-definite. However, $\mathcal{L}$ for a weighted directed graph does not have this property.

### B. Existing Consensus Algorithm

Consider vehicles with double-integrator dynamics given by

$$\dot{r}_i = v_i, \qquad \dot{v}_i = u_i, \quad i = 1, \ldots, n, \tag{1}$$

where $r_i \in \mathbb{R}^m$ and $v_i \in \mathbb{R}^m$ are, respectively, the position and velocity of the $i$th vehicle, and $u_i \in \mathbb{R}^m$ is the control input. A consensus algorithm for (1) is studied in [2], [10] as

$$u_i = -\sum_{j=1}^{n} a_{ij}(r_i - r_j) - \alpha v_i, \quad i = 1, \ldots, n, \tag{2}$$

where $a_{ij}$ is the $(i, j)$th entry of weighted adjacency matrix $\mathcal{A}$ associated with weighted directed graph $\mathcal{G}$, and $\alpha$ is a

positive gain. Consensus is reached using (2) if for all $r_i(0)$ and $v_i(0)$, $r_i(t) \to r_j(t)$ and $v_i(t) \to 0$ as $t \to \infty$.

### III. CONSENSUS FOR DOUBLE-INTEGRATOR DYNAMICS WITH CARTESIAN COORDINATE COUPLING

In this section, we consider a consensus algorithm for double-integrator dynamics (1) with Cartesian coordinate coupling as

$$u_i = -\sum_{j=1}^{n} a_{ij} C(r_i - r_j) - \alpha v_i, \quad i = 1, \dots, n, \quad (3)$$

where $C \in \mathbb{R}^{m \times m}$ denotes a Cartesian coordinate coupling matrix. Note that (2) corresponds to the case where $C = I_m$. That is, using (2), the components of $r_i$ (i.e., the Cartesian coordinates of vehicle $i$) are decoupled while using (3) the components of $r_i$ are coupled. In this section, we focuses on the case where $C$ is a rotation matrix while a similar analysis can be extended to the case where $C$ is a general matrix.

Before moving on, we need the following lemmas and definition:

*Lemma 3.1:* [11] Let $U \in \mathbb{R}^{p \times p}$, $V \in \mathbb{R}^{q \times q}$, $X \in \mathbb{R}^{p \times p}$, and $Y \in \mathbb{R}^{q \times q}$. Then $(U \otimes V)(X \otimes Y) = UX \otimes VY$. Let $A \in \mathbb{R}^{p \times p}$ have eigenvalues $\beta_i$ with associated eigenvectors $f_i \in \mathbb{C}^p$, $i = 1, \dots, p$, and let $B \in \mathbb{R}^{q \times q}$ have eigenvalues $\rho_j$ with associated eigenvectors $g_j \in \mathbb{C}^q$, $j = 1, \dots, q$. Then the $pq$ eigenvalues of $A \otimes B$ are $\beta_i \rho_j$ with associated eigenvectors $f_i \otimes g_j$, $i = 1, \dots, p$, $j = 1, \dots, q$.

*Lemma 3.2:* [12] Let $\mathcal{L}$ be the nonsymmetric Laplacian matrix associated with weighted directed graph $\mathcal{G}$. Then $\mathcal{L}$ has at least one zero eigenvalue and all nonzero eigenvalues have positive real parts. Furthermore, $\mathcal{L}$ has a simple zero eigenvalue and all other eigenvalues have positive real parts if and only if $\mathcal{G}$ has a directed spanning tree. In addition, there exist $\mathbf{1}_n$, where $\mathbf{1}_n$ is the $n \times 1$ column vector of all ones, satisfying $\mathcal{L}\mathbf{1}_n = 0$ and $\mathbf{p} \in \mathbb{R}^n$ satisfying $\mathbf{p} \geq 0$, $\mathbf{p}^T \mathcal{L} = 0$, and $\mathbf{p}^T \mathbf{1} = 1$.[1]

*Definition 3.1:* Let $\mu_i$, $i = 1, \dots, n$, be the $i$th eigenvalue of $-\mathcal{L}$ with associated right eigenvector $w_i$ and left eigenvector $\nu_i$. Also let $\arg(\mu_i) = 0$ for $\mu_i = 0$ and $\arg(\mu_i) \in (\frac{\pi}{2}, \frac{3\pi}{2})$ for all $\mu_i \neq 0$, where $\arg(\cdot)$ denotes the phase of a number. Without loss of generality, suppose that $\mu_i$ is labeled such that $\arg(\mu_1) \leq \arg(\mu_2) \leq \cdots \leq \arg(\mu_n)$.[2]

*Lemma 3.3:* (see e.g., [13]) Given a rotation matrix $R \in \mathbb{R}^{3 \times 3}$, let $\mathbf{a} = [a_1, a_2, a_3]^T$ and $\theta$ denote, respectively, the Euler axis (i.e., the unit vector in the direction of rotation) and Euler angle (i.e., the rotation angle). The eigenvalues of $R$ are $1$, $e^{\iota\theta}$, and $e^{-\iota\theta}$, where $\iota$ denotes the imaginary unit, with the associated right eigenvectors given by, respectively, $\varsigma_1 = \mathbf{a}$, $\varsigma_2 = [(a_2^2 + a_3^2)\sin^2(\frac{\theta}{2}), -a_1 a_2 \sin^2(\frac{\theta}{2}) + \iota a_3 \sin(\frac{\theta}{2})|\sin(\frac{\theta}{2})|, -a_1 a_3 \sin^2(\frac{\theta}{2}) - \iota a_2 \sin(\frac{\theta}{2})|\sin(\frac{\theta}{2})|]^T$, and $\varsigma_3 = \bar{\varsigma}_2$, where $\bar{\cdot}$ denotes the complex conjugate of a number. The associated left eigenvectors are, respectively, $\varpi_1 = \varsigma_1$, $\varpi_2 = \bar{\varsigma}_2$, and $\varpi_3 = \bar{\varsigma}_3$.

---

[1] That is, $\mathbf{1}_n$ and $\mathbf{p}$ are, respectively, the right and left eigenvectors of $\mathcal{L}$ associated with the zero eigenvalue.

[2] It follows from Lemma 3.2 that $\mu_1 = 0$, $w_1 = \mathbf{1}_n$, and $\nu_1 = \mathbf{p}$.

*Lemma 3.4:* Let $A \in \mathbb{R}^{n \times n}$ with eigenvalues $\gamma_i$ and associated right and left eigenvectors $q_i$ and $s_i$, respectively. Also let $B = \begin{bmatrix} 0_{n \times n} & I_n \\ A & -\alpha I_n \end{bmatrix}$, where $0_{n \times n}$ denotes the $n \times n$ zero matrix and $\alpha$ is a positive scalar. Then the eigenvalues of $B$ are given by $\zeta_{2i-1} = \frac{-\alpha + \sqrt{\alpha^2 + 4\gamma_i}}{2}$ with associated right and left eigenvectors $\begin{bmatrix} q_i \\ \zeta_{2i-1} q_i \end{bmatrix}$ and $\begin{bmatrix} (\zeta_{2i-1} + \alpha) s_i \\ s_i \end{bmatrix}$, respectively, and $\zeta_{2i} = \frac{-\alpha - \sqrt{\alpha^2 + 4\gamma_i}}{2}$, with associated right and left eigenvectors given by $\begin{bmatrix} q_i \\ \zeta_{2i} q_i \end{bmatrix}$ and $\begin{bmatrix} (\zeta_{2i} + \alpha) s_i \\ s_i \end{bmatrix}$, respectively,

*Proof:* Suppose that $\zeta$ is an eigenvalue of $B$ with an associated right eigenvector $\begin{bmatrix} f \\ g \end{bmatrix}$, where $f, g \in \mathbb{C}^n$. It follows that $\begin{bmatrix} 0_{n \times n} & I_n \\ A & -\alpha I_n \end{bmatrix} \begin{bmatrix} f \\ g \end{bmatrix} = \zeta \begin{bmatrix} f \\ g \end{bmatrix}$, which implies $g = \zeta f$ and $Af - \alpha g = \zeta g$. It thus follows that $Af = (\zeta^2 + \alpha\zeta)f$. Noting that $Aq_i = \gamma_i q_i$, we let $f = q_i$ and $\zeta^2 + \alpha\zeta = \gamma_i$. That is, each eigenvalue of $A$, $\gamma_i$, corresponds to two eigenvalues of $B$, denoted by $\zeta_{2i-1,2i} = \frac{-\alpha \pm \sqrt{\alpha^2 + 4\gamma_i}}{2}$. Because $g = \zeta f$, it follows that the right eigenvectors associated with $\zeta_{2i-1}$ and $\zeta_{2i}$ are, respectively, $\begin{bmatrix} q_i \\ \zeta_{2i-1} q_i \end{bmatrix}$ and $\begin{bmatrix} q_i \\ \zeta_{2i} q_i \end{bmatrix}$. A similar analysis can be used to find the left eigenvectors of $B$ associated with $\zeta_{2i-1}$ and $\zeta_{2i}$. ∎

*Theorem 3.2:* Suppose that weighted directed graph $\mathcal{G}$ has a directed spanning tree. Let the control algorithm for (1) be given by (3), where $r_i = [x_i, y_i, z_i]^T$ and $v_i = [v_{xi}, v_{yi}, v_{zi}]^T$. Let $\mu_i$, $w_i$, $\nu_i$, and $\arg(\mu_i)$ be defined in Definition 3.1, $\mathbf{p}$ be defined in Lemma 3.2, and $\mathbf{a} = [a_1, a_2, a_3]^T$, $\varsigma_k$, and $\varpi_k$ be defined in Lemma 3.3.

1) Suppose that $C = I_3$. Then all vehicles will eventually rendezvous if and only if $\alpha > \alpha^c$, where $\alpha^c \overset{\triangle}{=} \max_i \sqrt{\frac{|\mu_i| \sin^2(\arg(\mu_i))}{-\cos(\arg(\mu_i))}}$. The rendezvous position is given by

$$[\mathbf{p}^T (x(0) + \frac{v_x(0)}{\alpha}), \mathbf{p}^T (y(0) + \frac{v_y(0)}{\alpha}), \mathbf{p}^T (z(0) + \frac{v_z(0)}{\alpha})], \quad (4)$$

where $x$, $y$, $z$, $v_x$, $v_y$, and $v_z$ are, respectively, stack vectors of $x_i$, $y_i$, $z_i$, $v_{xi}$, $v_{yi}$, and $v_{zi}$.

2) Suppose that $C = R$, where $R$ is the $3 \times 3$ rotation matrix defined in Lemma 3.3, and $\alpha > \alpha^c$. Given $|\mu_i|$, $i = 2, \dots, n$, let $\psi_i^l \in (\frac{\pi}{2}, \pi)$ (respectively, $\psi_i^u \in (\pi, \frac{3\pi}{2})$) be the solution to $|\mu_i| \sin^2(\psi_i) + \alpha^2 \cos(\psi_i) = 0$ if $\arg(\mu_i) \in (\frac{\pi}{2}, \pi]$ (respectively, $\arg(\mu_i) \in [\pi, \frac{3\pi}{2})$). If $|\theta| < \theta_d^c$, where $\theta_d^c \overset{\triangle}{=} \min_{\arg(\mu_i) \in [\pi, \frac{3\pi}{2})}(\psi_i^u - \arg(\mu_i))$, then all vehicles will eventually rendezvous at the position given by (4).

3) Under the assumption of 2), if $|\theta| = \theta_d^c$ and there exists a unique $\arg(\mu_\kappa) \in [\pi, \frac{3\pi}{2})$ such that $\psi_\kappa^u - \arg(\mu_\kappa) = \theta_d^c$, then all vehicles will eventually move on circular orbits with center given by (4) and period $\frac{\pi\alpha}{|\mu_\kappa \sin(\psi_\kappa^u)|}$. The radius of the orbit for vehicle $i$ is given by $2|w_{\kappa(i)} p_c^T [r(0)^T, v(0)^T]^T| \sqrt{a_2^2 + a_3^2} \sin^2(\frac{\theta}{2})$, where $w_{\kappa(i)}$ is the $i$th component of $w_\kappa$ and

$$p_c = \frac{1}{(2\sigma_c+\alpha)\nu_\kappa^T w_\kappa \varpi_2^T \varsigma_2}\begin{bmatrix}(\sigma_c+\alpha)(\nu_\kappa\otimes\varpi_2)\\ \nu_\kappa\otimes\varpi_2\end{bmatrix}, \quad \text{where}$$

$\sigma_c = \iota\frac{2|\mu_\kappa||\sin(\psi_\kappa^u)|}{\alpha}$. The relative radius of the orbits is equal to the relative magnitude of $w_{\kappa(i)}$. The relative phase of the vehicles on their orbits is equal to the relative phase of $w_{\kappa(i)}$. The circular orbits are on a plane perpendicular to Euler axis $\mathbf{a}$.

4) If there exists a unique $\arg(\mu_\kappa) \in [\pi, \frac{3\pi}{2})$ such that $\psi_\kappa^u - \arg(\mu_\kappa) = \theta_d^c$ and $\theta_d^c < |\theta| < \min_{\arg(\mu_i)\in[\pi,\frac{3\pi}{2}),\ i\neq\kappa}(\psi_i^u - \arg(\mu_i))$, then the vehicles will eventually move along logarithmic spiral curves with center given by (4), growing rate $\mathrm{Re}(\sigma_s)$, where $\sigma_s = \frac{-\alpha+\sqrt{\alpha^2+4\lambda_s}}{2}$ with $\lambda_s = \mu_\kappa e^{\iota|\theta|}$, and period $\frac{2\pi}{|\mathrm{Im}(\sigma_s)|}$. The radius of the logarithmic spiral curve for vehicle $i$ is $2|w_{\kappa(i)}p_s^T[r(0)^T,v(0)^T]^T e^{\mathrm{Re}(\sigma_s)t}\sqrt{a_2^2+a_3^2}\sin^2(\frac{\theta}{2})$, where

$$p_s = \frac{1}{(2\sigma_s+\alpha)\nu_\kappa^T w_\kappa \varpi_2^T \varsigma_2}\begin{bmatrix}(\sigma_s+\alpha)(\nu_\kappa\otimes\varpi_2)\\ \nu_\kappa\otimes\varpi_2\end{bmatrix}.$$ The relative radius of the logarithmic spiral curves is equal to the relative magnitude of $w_{\kappa(i)}$. The relative phase of the vehicles on their curves is equal to the relative phase of $w_{\kappa(i)}$. The curves are on a plane perpendicular to Euler axis $\mathbf{a}$.

*Proof:* 1) For the first statement, if $C = I_3$, then (1) using (3) can be written in matrix form as

$$\begin{bmatrix}\dot{r}\\ \dot{v}\end{bmatrix} = \left(\underbrace{\begin{bmatrix}0_{n\times n} & I_n\\ -\mathcal{L} & -\alpha I_n\end{bmatrix}}_{\Gamma}\otimes I_3\right)\begin{bmatrix}r\\ v\end{bmatrix}, \tag{5}$$

where $r = [r_1^T,\ldots,r_n^T]^T$ and $v = [v_1^T,\ldots,v_n^T]^T$. It follows from the proof of Theorem 5.1 in [10] that the vehicles will eventually rendezvous if and only if $\Gamma$ defined in (5) has a simple zero eigenvalue and all other eigenvalues have negative real parts. Note from Lemma 3.4 that each eigenvalue $\mu_i$ of $-\mathcal{L}$ corresponds to two eigenvalues of $\Gamma$ given by $\zeta_{2i-1} = \frac{-\alpha+\sqrt{\alpha^2+4\mu_i}}{2}$ with associated right and left eigenvectors given by $\begin{bmatrix}w_i\\ \zeta_{2i-1}w_i\end{bmatrix}$ and $\begin{bmatrix}(\zeta_{2i-1}+\alpha)\nu_i\\ \nu_i\end{bmatrix}$, respectively, and $\zeta_{2i} = \frac{-\alpha-\sqrt{\alpha^2+4\mu_i}}{2}$, with associated right and left eigenvectors given by $\begin{bmatrix}w_i\\ \zeta_{2i}w_i\end{bmatrix}$ and $\begin{bmatrix}(\zeta_{2i}+\alpha)\nu_i\\ \nu_i\end{bmatrix}$, respectively, where $i=1,\ldots,n$.

Because weighted directed graph $\mathcal{G}$ has a directed spanning tree, it follows from Lemma 3.2 that $-\mathcal{L}$ has a simple zero eigenvalue and all other eigenvalues have negative real parts. According to Definition 3.1, we let $\mu_1 = 0$ and $\mathrm{Re}(\mu_i) < 0$, $i=2,\ldots,n$. Note from Lemma 3.2 that $w_1 = \mathbf{1}_n$ and $\nu_1 = \mathbf{p}$. It thus follows that $\zeta_1 = 0$ with associated right and left eigenvectors given by $\begin{bmatrix}\mathbf{1}_n\\ \mathbf{0}_n\end{bmatrix}$ and $\begin{bmatrix}\alpha\mathbf{p}\\ \mathbf{p}\end{bmatrix}$, respectively, and $\zeta_2 = -\alpha$. Note that $\zeta_2 < 0$ if $\alpha > 0$. Also noting that all $\sqrt{\alpha^2+4\mu_i}$ have nonnegative real parts, it follows that all $\zeta_{2i}$, $i=2,\ldots,n$, have negative real parts if $\alpha > 0$. It is left to show conditions under which $\zeta_{2i-1}$, $i=2,\ldots,n$, have negative real parts. Suppose that $\alpha_i^*$ is the critical value for $\alpha$ such that $\zeta_{2i-1}$, $i=2,\ldots,n$,

is on the imaginary axis. Let $\zeta_{2i-1} = \eta_i\iota$, where $\eta_i \in \mathbb{R}$, $i=2,\ldots,n$. After some manipulation, it follows that $\alpha_i^* = \sqrt{\frac{|\mu_i|\sin^2(\arg(\mu_i))}{-\cos(\arg(\mu_i))}}$ and $\eta_i = \frac{2|\mu_i|\sin(\arg(\mu_i))}{\alpha}$, $i=2,\ldots,n$. It is straightforward to verify that if $\alpha > \alpha_i^*$ (respectively, $\alpha < \alpha_i^*$), then $\zeta_{2i-1}$, $i=2,\ldots,n$, has a negative (respectively, positive) real part. Therefore, all $\zeta_{2i-1}$, $i=2,\ldots,n$, have negative real parts if and only if $\alpha > \max_{i=2,\ldots,n}\alpha_i^*$. Combining the above arguments shows that $\Gamma$ has a simple zero eigenvalue and all other eigenvalues have negative real parts if and only if $\alpha > \alpha^c$.

Note that $\Gamma$ can be written in Jordan canonical form as $SJS^{-1}$, where the columns of $S$, denoted by $s_k$, $k=1,\ldots,2n$, can be chosen to be the right eigenvectors or generalized right eigenvectors of $\Gamma$ associated with eigenvalue $\zeta_k$, $k=1,\ldots,2n$, the rows of $S^{-1}$, denoted by $h_k^T$, $k=1,\ldots,2n$, can be chosen to be the left eigenvectors or generalized left eigenvectors of $\Gamma$ associated with eigenvalue $\zeta_k$ such that $h_k^T s_k = 1$ and $h_k^T s_\ell = 0$, $k \neq \ell$, and $J$ is the Jordan block diagonal matrix with $\zeta_k$ being the diagonal entries. We can choose $s_1 = [\mathbf{1}_n^T, \mathbf{0}_n^T]^T$ and $h_1 = [\mathbf{p}^T, \frac{1}{\alpha}\mathbf{p}^T]^T$. Note that $h_1^T s_1 = 1$. It thus follows that $\lim_{t\to\infty}\begin{bmatrix}r(t)\\ v(t)\end{bmatrix} = \lim_{t\to\infty}(e^{\Gamma t}\otimes I_3)\begin{bmatrix}r(0)\\ v(0)\end{bmatrix} = \left[\left(\begin{bmatrix}\mathbf{1}_n\\ \mathbf{0}_n\end{bmatrix}\begin{bmatrix}\mathbf{p}^T & \frac{1}{\alpha}\mathbf{p}^T\end{bmatrix}\right)\otimes I_3\right]\begin{bmatrix}r(0)\\ v(0)\end{bmatrix}$, which implies that $x_i(t) \to \mathbf{p}^T x(0) + \frac{1}{\alpha}\mathbf{p}^T v_x(0)$, $y_i(t) \to \mathbf{p}^T y(0) + \frac{1}{\alpha}\mathbf{p}^T v_y(0)$, $z_i(t) \to \mathbf{p}^T z(0) + \frac{1}{\alpha}\mathbf{p}^T v_z(0)$, $v_{xi}(t) \to 0$, $v_{yi}(t) \to 0$, and $v_{zi}(t) \to 0$ as $t \to \infty$. Equivalently, it follows that all vehicles will eventually rendezvous at the position given by (4).

2) For the second statement, using (3), (1) can be written in matrix form as

$$\begin{bmatrix}\dot{r}\\ \dot{v}\end{bmatrix} = \underbrace{\begin{bmatrix}0_{3n\times 3n} & I_{3n}\\ -(\mathcal{L}\otimes R) & -\alpha I_{3n}\end{bmatrix}}_{\Sigma}\begin{bmatrix}r\\ v\end{bmatrix}. \tag{6}$$

It follows from Lemmas 3.1 and 3.3 and Definition 3.1 that the eigenvalues of $-(\mathcal{L}\otimes R)$ are $\mu_i$, $\mu_i e^{\iota\theta}$, and $\mu_i e^{-\iota\theta}$ with associated right eigenvectors $w_i\otimes\varsigma_1$, $w_i\otimes\varsigma_2$, and $w_i\otimes\varsigma_3$, respectively, and associated left eigenvectors $\nu_i\otimes\varpi_1$, $\nu_i\otimes\varpi_2$, and $\nu_i\otimes\varpi_3$, respectively. That is, the eigenvalues of $-(\mathcal{L}\otimes R)$ correspond to the eigenvalues of $-\mathcal{L}$ rotated by angles $0$, $\theta$, and $-\theta$, respectively. Let $\lambda_\ell$, $\ell=1,\ldots,3n$, denote the $\ell$th eigenvalue of $-(\mathcal{L}\otimes R)$. Without loss of generality, let $\lambda_{3i-2} = \mu_i$, $\lambda_{3i-1} = \mu_i e^{\iota\theta}$, and $\lambda_{3i} = \mu_i e^{-\iota\theta}$, $i=1,\ldots,n$, be the eigenvalues of $-(\mathcal{L}\otimes R)$. Note from Lemma 3.4 that each $\lambda_k$ corresponds to two eigenvalues of $\Sigma$, defined in (6), given by $\sigma_{2k-1,2k} = \frac{-\alpha\pm\sqrt{\alpha^2+4\lambda_k}}{2}$, $k=1,\ldots,3n$. Because $\mu_1 = 0$, it follows that $\lambda_1 = \lambda_2 = \lambda_3 = 0$, which in turn implies that $\sigma_1 = \sigma_3 = \sigma_5 = 0$ and $\sigma_2 = \sigma_4 = \sigma_6 = -\alpha$. Similar to the proof of the first statement, all $\sigma_{2k}$, $k=1,\ldots,3n$, have negative real parts if $\alpha > 0$. Given $\alpha > 0$ and $\chi_i = |\mu_i|e^{\iota\arg(\chi_i)}$, $i=2,\ldots,n$, $\psi_i^l$ and $\psi_i^u$ are the critical values for $\arg(\chi_i) \in [0, 2\pi)$ such that $\frac{-\alpha+\sqrt{\alpha^2+4\chi_i}}{2}$ is on the imaginary axis. In particular, if $\arg(\chi_i) = \psi_i^l$ (respectively, $\psi_i^u$), then $\frac{-\alpha+\sqrt{\alpha^2+4\chi_i}}{2} = \iota\frac{2|\mu_i||\sin(\arg(\psi_i^l))}{\alpha}$ (respectively,

$\iota\frac{2|\mu_i|\sin(\arg(\psi_i^u))}{\alpha}$), $i = 2,\ldots,n$. If $\arg(\chi_i) \in (\psi_i^l, \psi_i^u)$ (respectively, $\arg(\chi_i) \in [0, \psi_i^l) \cup (\psi_i^u, 2\pi)$), then $\frac{-\alpha+\sqrt{\alpha^2+4\chi_i}}{2}$ have negative (respectively, positive) real parts. Because $\alpha > \alpha^c$, the first statement implies that all $\frac{-\alpha+\sqrt{\alpha^2+4\mu_i}}{2}$, $i = 2,\ldots,n$, have negative real parts, which in turn implies that $\arg(\mu_i) \in (\psi_i^l, \psi_i^u)$, $i = 2,\ldots,n$. If $|\theta| < \theta_d^c$, then $\arg(\lambda_{3i-2})$, $\arg(\lambda_{3i-1})$, and $\arg(\lambda_{3i})$ are all within $(\psi_i^l, \psi_i^u)$, which implies that $\sigma_{6i-5}$, $\sigma_{6i-3}$, and $\sigma_{6i-1}$, $i = 2,\ldots,n$, all have negative real parts. Therefore, if $|\theta| < \theta_d^c$, then $\Sigma$ has exactly three zero eigenvalues and all other eigenvalues have negative real parts.

Similar to the proof of the first statement, we write $\Sigma$ in Jordan canonical form as $MJM^{-1}$, where the columns of $M$, denoted by $m_k$, $k = 1,\ldots,6n$, can be chosen to be the right eigenvectors or generalized right eigenvectors of $\Sigma$ associated with eigenvalue $\sigma_k$, the rows of $M^{-1}$, denoted by $p_k^T$, $k = 1,\ldots,6n$, can be chosen to be the left eigenvectors or generalized left eigenvectors of $\Sigma$ associated with eigenvalue $\sigma_k$ such that $p_k^T m_k = 1$ and $p_k^T m_\ell = 0$, $k \neq \ell$, and $J$ is the Jordan block diagonal matrix with $\sigma_k$ being the diagonal entries. Note that the right and left eigenvectors of $-(\mathcal{L} \otimes R)$ associated with eigenvalue $\lambda_\ell = 0$ are, respectively, $\mathbf{1}_n \otimes \varsigma_\ell$ and $\mathbf{p} \otimes \varpi_\ell$, where $\ell = 1, 2, 3$. It in turn follows from Lemma 3.4 that the right and left eigenvectors of $\Sigma$ associated with $\sigma_{2\ell-1} = 0$ are, respectively, $\begin{bmatrix} \mathbf{1}_n \otimes \varsigma_\ell \\ \mathbf{0}_{3n} \end{bmatrix}$ and $\begin{bmatrix} \alpha\mathbf{p} \otimes \varpi_\ell \\ \mathbf{p} \otimes \varpi_\ell \end{bmatrix}$, where $\ell = 1, 2, 3$. We can choose $m_{2\ell-1} = \begin{bmatrix} \mathbf{1}_n \otimes \varsigma_\ell \\ \mathbf{0}_{3n} \end{bmatrix}$ and $p_{2\ell-1} = \begin{bmatrix} \mathbf{p} \otimes \frac{\varpi_\ell}{\varpi_\ell^T \varsigma_\ell} \\ \mathbf{p} \otimes \frac{\varpi_\ell}{\alpha\varpi_\ell^T \varsigma_\ell} \end{bmatrix}$, where $\ell = 1, 2, 3$. Note that $p_{2\ell-1}^T m_{2\ell-1} = 1$ and $p_{2\ell-1}^T m_{2k-1} = 0$, where $k, \ell = 1, 2, 3$ and $k \neq \ell$. Noting that $\sigma_{2\ell-1} = 0$, $\ell = 1, 2, 3$, it follows that $\lim_{t\to\infty} \begin{bmatrix} r(t) \\ v(t) \end{bmatrix} = \lim_{t\to\infty} Me^{Jt}M^{-1}\begin{bmatrix} r(0) \\ v(0) \end{bmatrix} \to (\sum_{\ell=1}^3 m_{2\ell-1}p_{2\ell-1}^T)\begin{bmatrix} r(0) \\ v(0) \end{bmatrix}$, which implies that $x_i(t) \to \mathbf{p}^T x(0) + \frac{1}{\alpha}\mathbf{p}^T v_x(0)$, $y_i(t) \to \mathbf{p}^T y(0) + \frac{1}{\alpha}\mathbf{p}^T v_y(0)$, $z_i(t) \to \mathbf{p}^T z(0) + \frac{1}{\alpha}\mathbf{p}^T v_z(0)$, $v_{xi}(t) \to 0$, $v_{yi}(t) \to 0$, and $v_{zi}(t) \to 0$ as $t \to \infty$. Equivalently, it follows that all vehicles will eventually rendezvous at the position given by (4).

3) For the third statement, if $\theta = \theta_d^c$ (respectively, $\theta = -\theta_d^c$) and there exists a unique $\arg(\mu_\kappa) \in [\pi, \frac{3\pi}{2})$ such that $\psi_\kappa^u - \arg(\mu_\kappa) = \theta_d^c$, then $\lambda_{3\kappa-1} = \mu_\kappa e^{\iota\theta} = |\mu_\kappa|e^{\iota\psi_\kappa^u}$ (respectively, $\lambda_{3\kappa} = \mu_\kappa e^{-\iota\theta} = |\mu_\kappa|e^{\iota\psi_\kappa^u}$), which implies that $\sigma_{6\kappa-3} = \frac{-\alpha+\sqrt{\alpha^2+4\lambda_{3\kappa-1}}}{2} = \iota\frac{2|\mu_\kappa|\sin(\psi_\kappa^u)}{\alpha}$ (respectively, $\sigma_{6\kappa-1} = \frac{-\alpha+\sqrt{\alpha^2+4\lambda_{3\kappa}}}{2} = \iota\frac{2|\mu_\kappa|\sin(\psi_\kappa^u)}{\alpha}$). Noting that the complex eigenvalues of $\Sigma$ are in pairs, it follows that $\Sigma$ has an eigenvalue equal to $\overline{\sigma_{6\kappa-3}} = -\iota\frac{2|\mu_\kappa|\sin(\psi_\kappa^u)}{\alpha}$ (respectively, $\overline{\sigma_{6\kappa-1}} = -\iota\frac{2|\mu_\kappa|\sin(\psi_\kappa^u)}{\alpha}$), denoted by $\sigma_*$ for simplicity. In this case, $\Sigma$ has exactly three zero eigenvalues, two nonzero eigenvalues on the imaginary axis, and all other eigenvalues have negative real parts. In the following, we focus on $\theta = \theta_d^c$ since the analysis for $\theta = -\theta_d^c$ is similar except that all vehicles will move in reverse

directions. Note from Lemma 3.4 that the right and left eigenvectors associated with $\sigma_{6\kappa-3}$ are, respectively, $\begin{bmatrix} w_\kappa \otimes \varsigma_2 \\ \sigma_{6\kappa-3}(w_\kappa \otimes \varsigma_2) \end{bmatrix}$ and $\begin{bmatrix} (\sigma_{6\kappa-3} + \alpha)(\nu_\kappa \otimes \varpi_2) \\ \nu_\kappa \otimes \varpi_2 \end{bmatrix}$. We can choose $m_{6\kappa-3} = \begin{bmatrix} w_\kappa \otimes \varsigma_2 \\ \sigma_{6\kappa-3}(w_\kappa \otimes \varsigma_2) \end{bmatrix}$ and $p_{6\kappa-3} = \frac{1}{(2\sigma_{6\kappa-3}+\alpha)\nu_\kappa^T w_\kappa \varpi_2^T \varsigma_2}\begin{bmatrix} (\sigma_{6\kappa-3} + \alpha)(\nu_\kappa \otimes \varpi_2) \\ \nu_\kappa \otimes \varpi_2 \end{bmatrix}$. Note that $p_{6\kappa-3}^T m_{6\kappa-3} = 1$. Similarly, it follows that $m_*$ and $p_*$ corresponding to $\sigma_*$ are given by $m_* = \overline{m_{6\kappa-3}}$ and $p_* = \overline{p_{6\kappa-3}}$. It follows that $\begin{bmatrix} r(t) \\ v(t) \end{bmatrix} = e^{\Sigma t}\begin{bmatrix} r(0) \\ v(0) \end{bmatrix} \to (\sum_{\ell=1}^3 m_{2\ell-1}p_{2\ell-1}^T)\begin{bmatrix} r(0) \\ v(0) \end{bmatrix} + c(t)$ for large $t$, where $c(t) \triangleq (e^{\iota\frac{2|\mu_\kappa|\sin(\psi_\kappa^u)}{\alpha}t}m_{6\kappa-3}p_{6\kappa-3}^T + e^{-\iota\frac{2|\mu_\kappa|\sin(\psi_\kappa^u)}{\alpha}t}m_*p_*^T)\begin{bmatrix} r(0) \\ v(0) \end{bmatrix}$. Let $c_k(t)$ be the $k$th component of $c(t)$, $k = 1,\ldots,6n$. It follows that $c_{3(i-1)+\ell}(t) = 2\text{Re}(e^{\iota\frac{2|\mu_\kappa|\sin(\psi_\kappa^u)}{\alpha}t}w_{\kappa(i)}\varsigma_{2(\ell)}p_{6\kappa-3}^T[r(0)^T, v(0)^T]^T)$, where $i = 1,\ldots,n$, $\ell = 1, 2, 3$, and $\varsigma_{2(\ell)}$ denotes the $\ell$th component of $\varsigma_2$. After some manipulation, it follows that $c_{3(i-1)+\ell}(t) = 2|\varsigma_{2(\ell)}w_{\kappa(i)}p_{6\kappa-3}^T[r(0)^T, v(0)^T]^T| \cos(\frac{2|\mu_\kappa|\sin(\psi_\kappa^u)}{\alpha}t + \arg(w_{\kappa(i)}p_{6\kappa-3}^T[r(0)^T, v(0)^T]^T) + \arg(\varsigma_{2(\ell)}))$, $i = 1,\ldots,n$, $\ell = 1, 2, 3$. Therefore, it follows that $x_i(t) \to \mathbf{p}^T x(0) + \frac{1}{\alpha}\mathbf{p}^T v_x(0) + c_{3i-2}(t)$, $y_i(t) \to \mathbf{p}^T y(0) + \frac{1}{\alpha}\mathbf{p}^T v_y(0) + c_{3i-1}(t)$, and $z_i(t) \to \mathbf{p}^T z(0) + \frac{1}{\alpha}\mathbf{p}^T v_z(0) + c_{3i}(t)$ for large $t$. After some manipulation, it can be verified that $\|[c_{3i-2}(t), c_{3i-1}(t), c_{3i}(t)]^T\| = 2|w_{\kappa(i)}p_{6\kappa-3}^T[r(0)^T, v(0)^T]^T|\sqrt{a_2^2 + a_3^2}\sin^2(\frac{\theta}{2})$, which is a constant. Therefore, it follows that all vehicles will eventually move on circular orbits with center give by (4) and period $\frac{\pi\alpha}{|\mu_\kappa \sin(\psi_\kappa^u)|}$. The radius of the orbit for vehicle $i$ is given by $2|w_{\kappa(i)}p_{6\kappa-3}^T[r(0)^T, v(0)^T]^T|\sqrt{a_2^2 + a_3^2}\sin^2(\frac{\theta}{2})$. The relative radius of the orbits is equal to the relative magnitude of $w_{\kappa(i)}$. In addition, the relative phase of the vehicles is equal to the relative phase of $w_{\kappa(i)}$. Note from Lemma 3.3 that Euler axis $\mathbf{a}$ is orthogonal to both $\text{Re}(\varsigma_2)$ and $\text{Im}(\varsigma_2)$, where $\text{Re}(\cdot)$ and $\text{Im}(\cdot)$, representing, respectively, the real and imaginary part of a number, are applied componentwise. It can thus be verified that $\mathbf{a}$ is orthogonal to $[c_{3i-2}(t), c_{3i-1}(t), c_{3i}(t)]^T$, which implies that the circular orbits are on a plane perpendicular to $\mathbf{a}$.

4) For the fourth statement, if there exists a unique $\arg(\mu_\kappa) \in [\pi, \frac{3\pi}{2})$ such that $\psi_\kappa^u - \arg(\mu_\kappa) = \theta_d^c$ and $\theta_d^c < \theta < \min_{\arg(\mu_i)\in[\pi,\frac{3\pi}{2}), i\neq\kappa}(\psi_i^u - \arg(\mu_i))$ (respectively, $-\min_{\arg(\mu_i)\in[\pi,\frac{3\pi}{2}), i\neq\kappa}(\psi_i^u - \arg(\mu_i)) < \theta < -\theta_d^c$), then $\lambda_{3\kappa-1} = \mu_\kappa e^{\iota\theta} = |\mu_\kappa|e^{\iota(\arg(\mu_\kappa)+\theta)}$ (respectively, $\lambda_{3\kappa} = \mu_\kappa e^{-\iota\theta} = |\mu_\kappa|e^{\iota(\arg(\mu_\kappa)-\theta)}$), where $\arg(\mu_\kappa) + \theta > \psi_\kappa^u$ (respectively, $\arg(\mu_\kappa) - \theta > \psi_\kappa^u$), which implies that $\sigma_{6\kappa-3} = \frac{-\alpha+\sqrt{\alpha^2+4\lambda_{3\kappa-1}}}{2}$ (respectively, $\sigma_{6\kappa-1} = \frac{-\alpha+\sqrt{\alpha^2+4\lambda_{3\kappa}}}{2}$) has a positive real part. A similar argument as above shows that $\Sigma$ has exactly three zero eigenvalues and two eigenvalues with positive real parts and all other eigenvalues have negative real parts. By following a similar procedure to the proof of the third statement, we can show that all vehicles will eventually move along

logarithmic spiral curves with center given by (4), growing rate $\text{Re}(\sigma_{6\kappa-3})$, and period $\frac{2\pi}{|\text{Im}(\sigma_{6\kappa-3})|}$. The radius of the logarithmic spiral curve for vehicle $i$ is given by $2|w_{\kappa(i)}p_{6\kappa-3}^T[r(0)^T, v(0)^T]^T|e^{\text{Re}(\sigma_{6\kappa-3})t}\sqrt{a_2^2 + a_3^2}\sin^2(\frac{\theta}{2})$. The relative radius of the logarithmic spiral curves is equal to the relative magnitude of $w_{\kappa(i)}$. In addition, the relative phase of the vehicles on their curves is equal to the relative phase of $w_{\kappa(i)}$. A similar argument to that for the third statement shows that the curves are on a plane perpendicular to Euler axis $\mathbf{a}$. ∎

*Remark 3.3:* Note that the first statement of Theorem 3.2 generalizes Theorem 5.1 in [10], which gives only a sufficient condition for $\alpha$, by giving a necessary and sufficient condition. Unlike the single-integrator case, the critical value for the Euler angle for double-integrator dynamics depend on both $\alpha$ and $\mathcal{L}$. The critical value for the Euler angle in the double-integrator case is smaller than that for the single-integrator case. When $\alpha$ increases to infinity, the critical value for the Euler angle in the double-integrator case approaches that for the single-integrator case. Note that besides the network topology and the Euler angle, $\alpha$ plays an important role in (3).

*Example 3.4:* To illustrate, consider four vehicles with network topology $\mathcal{G}$ shown by Fig. 1. Let $\mathcal{L}$ associated with $\mathcal{G}$ be given by

$$\begin{bmatrix} 1.5 & 0 & -1.1 & -0.4 \\ -1.2 & 1.2 & 0 & 0 \\ -0.1 & -0.5 & 0.6 & 0 \\ -1 & 0 & 0 & 1 \end{bmatrix}. \quad (7)$$

It can be computed that $\theta_d^c = 0.3557$ rad. Let $R$ be the rotation matrix corresponding to Euler axis $\mathbf{a} = \frac{1}{14}[1, 2, 3]^T$ and Euler angle $\theta = \theta_d^c$. Fig. 2 shows the eigenvalues of $-\mathcal{L}$ and $-(\mathcal{L} \otimes R)$. Note that the eigenvalues of $-(\mathcal{L} \otimes R)$ correspond to the eigenvalues of $-\mathcal{L}$ rotated by angles 0, $\theta$, and $-\theta$. Fig. 3 shows the eigenvalues of $\Sigma$. Note that each eigenvalue of $-(\mathcal{L} \otimes R)$, $\lambda_k$, correspond to two eigenvalues of $\Sigma$, $\sigma_{2k-1,2k}$, where $\sigma_{2k-1,2k} = \frac{-\alpha \pm \sqrt{\alpha^2 + 4\lambda_k}}{2}$, $k = 1, \ldots, 12$. Because $\theta = \theta_d^c$, two nonzero eigenvalues of $\Sigma$ are located on the imaginary axis as shown in Fig. 2.
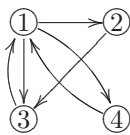


Fig. 1. Network topology for four vehicles. An arrow from $j$ to $i$ denotes that vehicle $i$ can receive information from vehicle $j$.

## IV. SIMULATION

In this section, we study collective motions of four vehicles using (3). Suppose that the network topology is given by Fig. 1 and $\mathcal{L}$ is given by (7). Let $\theta_s^c$, $\theta_d^c$, and $\mathbf{a}$ be given in Example 3.4. Using (3), it can be computed that $\alpha^c = 0.3626$. We let $\alpha = \alpha^c + 0.5$. Also note that there exists
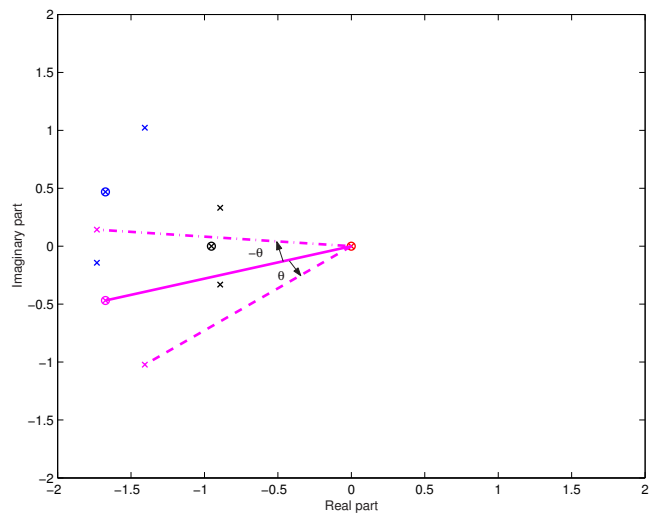


Fig. 2. Eigenvalues of $-\mathcal{L}$ and $-(\mathcal{L} \otimes R)$ with $\theta = \theta_d^c$. Circles denote the eigenvalues of $-\mathcal{L}$ while x-marks denote the eigenvalues of $-(\mathcal{L} \otimes R)$. The eigenvalues of $-(\mathcal{L} \otimes R)$ correspond to the eigenvalues of $-\mathcal{L}$ rotated by angles 0, $\theta$, and $-\theta$, respectively. In particular, the eigenvalues obtained by rotating $\mu_4$ by angles 0, $\theta$, and $-\theta$ are shown by, respectively, the solid line, the dashed line, and the dashdot line.

a unique $\arg(\mu_4) \in [\pi, \frac{3\pi}{2})$ such that $\psi_4^u - \arg(\mu_4) = \theta_d^c$ (i.e., $\kappa = 4$ in Theorem 3.2). Note that the right eigenvector of $-\mathcal{L}$ associated with eigenvalue $\mu_4$ is $w_4 = [-0.2847 - 0.2820\iota, 0.7213, -0.2501 + 0.1355\iota, 0.4809 + 0.0837\iota]^T$. Also note that $\mathbf{p} = [0.2502, 0.1911, 0.4587, 0.1001]^T$.

Figs. 4, 5, and 6 show, respectively, the trajectories of the four vehicles using (3) with $\theta = \theta_d^c - 0.2$, $\theta = \theta_d^c$, and $\theta = \theta_d^c + 0.2$. Note that all vehicles eventually rendezvous at the position given by (4) when $\theta = \theta_d^c - 0.2$, move on circular orbits when $\theta = \theta_d^c$, and move along logarithmic spiral curves when $\theta = \theta_d^c + 0.2$. Also note that when $\theta = \theta_d^c$, the relative radius of the circular orbits (respectively, the relative phase of the vehicles) is equal to the relative magnitude (respectively, phase) of the components of $w_4$. In addition, the trajectories of all vehicles are perpendicular to Euler axis $\mathbf{a}$ in all cases. By comparing the simulation results with those in [9], we note that the critical values for the Euler angle, the period of the circular motion, and the period and growing rate of the logarithmic spiral motion are quite different in both cases even if the network topology and $\mathcal{L}$ are chosen to the same in both cases.

## V. CONCLUSION

We have introduced Cartesian coordinate coupling to a consensus algorithm by a rotation matrix in 3D for double-integrator dynamics. The results generalize the results presented in the first part [9] of the two-part paper and existing results on consensus algorithms for double-integrator dynamics. We have shown that the network topology, the damping gain, and the value of the Euler angle all affect the resulting collective motions and quantitatively characterize the resulting collective motions. Simulation results have shown the effectiveness of theoretical results.
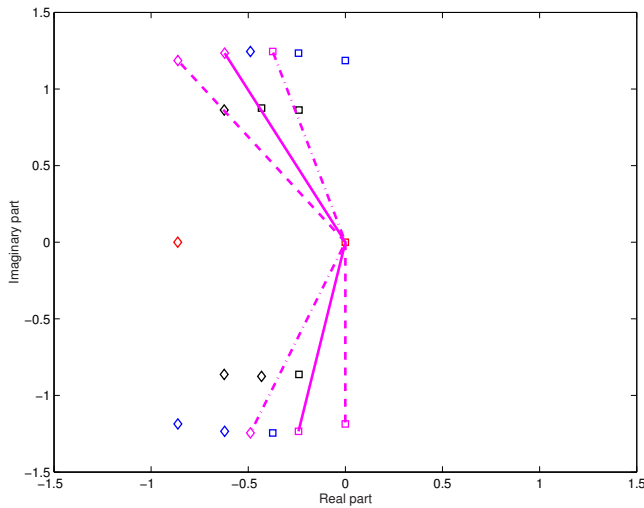
Fig. 3.　Eigenvalues of $\Sigma$ with $\theta = \theta_d^c$. Squares denote the eigenvalues computed by $\sigma_{2k-1} = \frac{-\alpha + \sqrt{\alpha^2 + 4\lambda_k}}{2}$ while diamonds denote the eigenvalues computed by $\sigma_{2k} = \frac{-\alpha - \sqrt{\alpha^2 + 4\lambda_k}}{2}$, $k = 1, \ldots, 12$. In particular, the eigenvalues of $\Sigma$ correspond to $\lambda_{10} = \mu_4$, $\lambda_{11} = \mu_4 e^{\iota\theta}$, and $\lambda_{12} = \mu_4 e^{-\iota\theta}$ are shown by, respectively, the solid line, the dashed line, and the dashdot line. Because $\theta = \theta_d^c$, two nonzero eigenvalues of $\Sigma$ are on the imaginary axis.
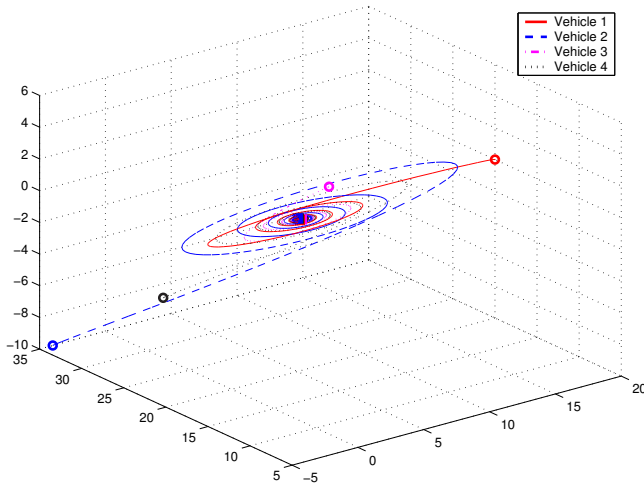


Fig. 4.　Trajectories of the four vehicles using (3) with $\theta = \theta_d^c - 0.2$. Circles denote the starting positions of the vehicles while the squares denote the snapshots of the vehicles at 30 sec.



Fig. 5.　Trajectories of the four vehicles using (3) with $\theta = \theta_d^c$. Circles denote the starting positions of the vehicles while the squares denote the snapshots of the vehicles at 30 sec.
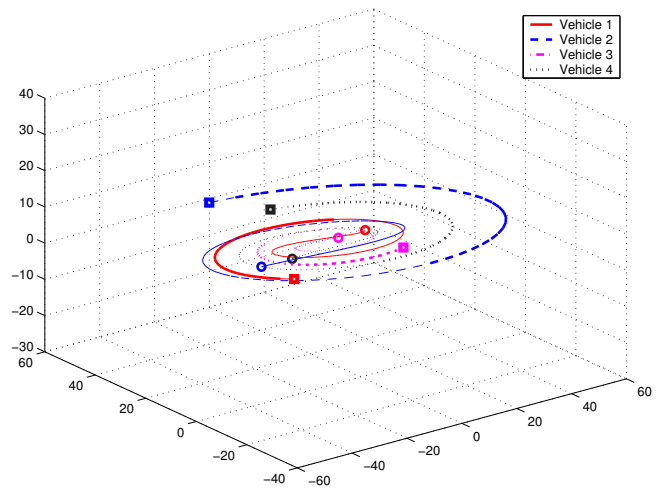


Fig. 6.　Trajectories of the four vehicles using (3) with $\theta = \theta_d^c + 0.2$. Circles denote the starting positions of the vehicles while the squares denote the snapshots of the vehicles at 10 sec.

## REFERENCES

[1] W. Ren and E. M. Atkins, "Distributed multi-vehicle coordinated control via local information exchange," *International Journal of Robust and Nonlinear Control*, vol. 17, no. 10–11, pp. 1002–1033, July 2007.

[2] G. Xie and L. Wang, "Consensus control for a class of networks of dynamic agents," *International Journal of Robust and Nonlinear Control*, vol. 17, no. 10-11, pp. 941–959, July 2007.

[3] G. Lafferriere, A. Williams, J. Caughman, and J. J. P. Veerman, "Decentralized control of vehicle formations," *Systems and Control Letters*, vol. 54, no. 9, pp. 899–910, 2005.

[4] R. Olfati-Saber, "Flocking for multi-agent dynamic systems: Algorithms and theory," *IEEE Transactions on Automatic Control*, vol. 51, no. 3, pp. 401–420, March 2006.

[5] H. G. Tanner, A. Jadbabaie, and G. J. Pappas, "Flocking in fixed and switching networks," *IEEE Transactions on Automatic Control*, vol. 52, no. 5, pp. 863–868, May 2007.

[6] D. Lee and M. W. Spong, "Stable flocking of multiple inertial agents on balanced graphs," *IEEE Transactions on Automatic Control*, vol. 52, no. 8, pp. 1469–1475, August 2007.

[7] M. Pavone and E. Frazzoli, "Decentralized policies for geometric pattern formation and path coverage," *ASME Journal of Dynamic Systems, Measurement, and Control*, vol. 129, no. 5, pp. 633–643, September 2007.

[8] W. Ren, "Collective motion from consensus with Cartesian coordinate coupling - part i: Single-integrator kinematics," in *Proceedings of the IEEE Conference on Decision and Control*, 2008.

[9] ——, "On consensus algorithms for double-integrator dynamics," in *Proceedings of the IEEE Conference on Decision and Control*, New Orleans, LA, December 2007, pp. 2295–2300.

[10] A. J. Laub, *Matrix Analysis for Scientists and Engineers*.　Philadelphia, PA: SIAM, 2005.

[11] W. Ren and R. W. Beard, "Consensus seeking in multiagent systems under dynamically changing interaction topologies," *IEEE Transactions on Automatic Control*, vol. 50, no. 5, pp. 655–661, May 2005.

[12] http://www.mathpages.com/home/kmath593/kmath593.htm.